RSC Advances

ROYAL SOCIETY OF CHEMISTRY

www.rsc.org/advances

Curcumin loaded nanographene oxide reinforced fish scale collagen - A 3D scaffold biomaterial for wound healing application

Tapas Mitra[1], Piyali Jana Manna[1], S.T.K.Raja[2], A. Gnanamani[2], P.P.Kundu[1*]

[1] Department of Polymer Science & Technology, University of Calcutta, University College of Science & Technology, 92, A.P.C road, Kolkata – 700009, West Bengal (India).

[2] Microbiology Division, CSIR-Central Leather Research Institute, Adyar, Chennai 600020, Tamil Nadu (India)

*- Corresponding Authors

E mail: ppk923@yahoo.com (Prof. P.P.Kundu)

Abstract

In recent years, functionalization of graphene oxide (GO) is a challenging task to make GO as a potential candidate in biomedical field. GO refers to one-atom thick planar sheet of sp^2-bonded carbon atoms with functional groups containing oxygen attached to both the sides and area of the flake. Nowadays, functionalized GO has attracted significant research interest based on their application potential in different fields including biomedicine. In the present work we have prepared highly stabilized nano graphene oxide (NGO) in aqueous media. Followed by stabilization, NGO is functionalized with type I collagen (with the ratio of 2:1, NGO and collagen) to make a 3D scaffold as a novel platform for better tissue engineering (TE) research. The functionalization of NGO is achieved by grafting process, an innovative route to modify the properties of NGO. The size of the prepared NGO is measured by dynamic light scattering measurement and collagen functionalized NGO is characterized by X-ray diffraction, attenuated total reflectance (ATR) FT-IR, ultraviolet visible (UV-vis), atomic force microscopy (AFM) and Raman spectroscopy which confirm the oxidation of graphite flake to NGO and functionalization with collagen. The surface property of the collagen functionalized NGO (CFNGO) is characterized by employing the transmission electron microscopy (TEM) and scanning electron microscopy (SEM). The mechanical stability of the CFNGO is three times greater than that of the native collagen. *In vitro* cell line study reveals non toxicity of the CFNGO against NIH 3T3 fibroblast cell line. The antimicrobial study of curcumin loaded CFNGO displays the growth inhibition against gram +ve and gram –ve organisms at a considerable level whereas *in vivo* wound healing studies explored the faster wound healing efficiency of curcumin loaded CFNGO scaffold than that of collagen alone. These findings suggest that the curcumin loaded CFNGO could be serving as a better platform for wound healing application.

Keywords: Graphene oxide; Collagen; Scaffold; Mechanical stability; Thermal stability; Tissue engineering

1. INTRODUCTION

The major aim of TE is to restore or regenerate tissues and organs by biomimetic fabrication of scaffolds with similar structure and functionality to the extracellular matrix[1]. There has been an enormous progress in TE in recent years and over the past two decades; many techniques have been developed to design suitable scaffolds for tissue repairing. The role of the scaffold is to modulate differentiation and growth behaviors of, and to control the attachment and sitting patterns, of cells.

Collagen, an extracellular protein abundant in animal tissues, is of great interest in TE because of its biological origin, excellent biodegradability and biocompatibility. These characteristics have also contributed to the safe use of collagen in biomedical applications[2, 3]. Although it has been one of the most preferred biomaterials for *in vivo* medical applications, the difficult processing and poor mechanical properties have been the barriers to its use in biomedical and engineering applications. To improve the poor mechanical properties of collagen reinforcement with fillers or cross-linking has been often used, although the presence of residual cross-linking agents could lead to toxic side effects[4]. Among the various types, type I collagen has been extensively used as TE scaffolds and wound dressing systems due to its low antigenic and high direct cell adhesion properties. At present, the main sources of type I collagen are bovine or porcine dermis[5]. However, due to Bovine Spongiform Encephalopathy (BSE), Transmissible Spongiform Encephalopathy (TSE), Foot and Mouth Disease (FMD) in pigs and cattle the use of collagen and collagen derived products from these sources have been limited[6]. Type I collagen has also been extracted from skin, bone, fins, and scales of fresh water and

marine fishes, chicken skin and different marine animals like squid, octopus, jellyfish, starfish, etc[7-11]. Collagen from these sources was evaluated for their potential application as an alternative to mammalian collagen.

Graphene oxide (GO) is a graphene sheet with carboxylic groups at its edges and phenol hydroxyl and epoxide groups on its basal plane[12]. It has been reported that GO, is a good TE substrate due to its unique physicochemical properties, including large surface area, high dispersibility and hydrophilicity[13]. GO can promote biological interactions due to its many surface functional groups[14, 15]. Several investigators have reported that GO can serve as a carrier for drugs and other biomolecules[16, 17]. In addition, GO regulates the proliferation and differentiation of cultured mesenchymal stem cells[18-20]. GO will likely be used in combination with other materials[21-23] or growth factors[24, 25] in future medical applications, playing a facilitative role with other TE materials. Furthermore, nano sized graphene oxide (NGO) has been widely investigated for biomedical applications due to its unique physical, mechanical, and optical properties[26, 27]. The said beneficial effect suggested that if GO has been properly exploited it would solve most of the challenges of clinicians. If collagen has been functionalized with GO, the resulting GO-collagen scaffold can efficiently deliver both hydrophobic and hydrophilic drugs simultaneously, because hydrophobic drug can be tethered with GO with π-π interaction, whereas, the hydrophilic drug can be interacted with collagen through its free primary amine and carboxylic functional groups. The diverse functional groups in GO-Collagen scaffold, further facilitates the conjugation of growth factors, DNA, SiRNA, etc., and implied the suitability for multiple targeted drug delivery system, which is in demand currently.

Curcumin (diferuloylmethane) is an orange-yellow component of perennial herb *Curcuma longa*. Curcumin is a naturally occurring multifunctional polyphenolic phytoconstituent which presents

anti-inflammatory[28], antimicrobial[29], antiviral[30], anticancer[31], antioxidant[32], and wound healing activities[33]. Despite all these promising features, a common problem with curcumin is the very low solubility in aqueous solutions, which limits its bioavailability and clinical efficacy. To overcome the problems of solubility and bioavailability of curcumin, the development of novel delivery systems is attracting significant attention in recent past[34]. One of the method is topical formulation of curcumin to support dermal wound healing[35]. Topical applications of curcumin provides antibacterial, anti-inflammatory, antioxidant (free radical scavenging activity) and protection against degenerative disease in patients have shown to improve significantly wound healing and protect tissues from oxidative damage[35]. Therefore, development of novel curcumin delivery systems is required.

In the present study we have selected a model hydrophobic drug curcumin to show the ionic as well as π-π stacking interaction between curcumin and GO-Collagen scaffold. After the incorporation of the drug either the material can be used as a wound healing material has also been explored in the present study.

Thus, the present work has been designed to; (i) improve the mechanical properties of collagen by reinforcing NGO; (ii) proper exploitation of the functional groups (oxygen-containing groups including hydroxyls, epoxides, diols, ketones and carboxyl on the surface) of NGO for the conjugation of hydrophobic drug and finally (iii) to have a suitable TE material for wound healing applications.

2. EXPERIMENTAL SECTION

2.1. Materials

All the major reagents used in this research were as follows: Graphite Nanopowder (Type 1) was purchased from Sisco research laboratories pvt.ltd. (India); N-(3-dimethylaminopropyl)-

N'-ethylcarbodiimide) hydrochloride (EDC HCl), and N-Hydroxysuccinimide (NHS), picrylsulfonic acid [2, 4, 6-trinitrobenzene sulfonic acid (TNBS)], 3-(4,5-dimethylthiazol-2-yl)-2,5-diphenyl- tetrazolium bromide (MTT), dialysis bags (MWCO = 14,000), curcumin were purchased from Sigma–Aldrich Co.; 2-(N –morpholino) ethanesulfonic acid (MES buffer) was obtained from HiMedia (India); DMEM cell culture medium, fetal bovine serum (FBS), Calcein AM, a cell-permeant dye were purchased from Invitrogen, India. All of the other reagents were of analytical reagent grade and used as received.

2.2. Preparation of Graphene Oxide Sheets

Graphite nanopowder was oxidized to nano graphite oxide according to method followed by Hummers[36] with slight modification. In brief, to a 1000 mL beaker, graphite (0.5g), $NaNO_3$ (0.25g), and concentrated H_2SO_4 (50 mL) were added and stirred vigorously in an ice bath. After dissolution of the sodium nitrate, solid $KMnO_4$ (1.5 g) was added slowly and continue the stirring over 30 min to prevent dangerous overheating (i.e.,>30°C). Upon addition of all $KMnO_4$, the ice bath was replaced with an oil bath (35-38°C) and the solution was stirred vigorously for next 3.5 h. During this time, the solution became highly viscous and turned dark brown. The reaction flask was then cooled in an ice bath, and double distilled water (75 mL) was slowly added to the solution, ensuring that the temperature remained below 40°C and stirred for another 2 h and 40 mL of 5% H_2O_2 was added, yielding a light yellow suspension of nano graphite oxide. The resulting graphite oxide was purified by three cycles of centrifugation (5500 rpm 15 min in centrifuge model REMI R-8C, INDIA), at first decantation, and resuspension in 5% H_2SO_4 and centrifuge in second step, freshly prepared 5% H_2O_2 was added to the precipitate collected from the first step and washed thoroughly and centrifuged. One M HCl was added to the precipitate collected from the second step and centrifuged. In the following step, the precipitate was washed for five times with distilled water. The as-synthesized purified graphite oxide was suspended in

double distilled water (100 mL) and exfoliated into individual graphene oxide nano sheets using a titanium-alloy solid probe ultrasonicator (125 W QsonicaSonicators Q125 Sonicator, Qsonica, LLC, Newtown, CT, USA) set at 40% intensity for of 6 h ON time. Any residual unexfoliated graphite oxide was removed by centrifugation at 5500 RPM for 20 min with the precipitate discarded. The resulting GO solution was then dialyzed double distilled water to remove the remaining salts (water changed every 4 h during daytime or after overnight).

2.3. Double Oxidation of Graphene Oxide

An aqueous dispersion of as-prepared GO was lyophilized and (OPERON FDU-8606, 6Liter, KOREA) the water free dried GO sample (0.5 g) was subjected again to the oxidation process as described above with proper scaling of all other reagents. All the other operations were repeated as described above to have double oxidized GO.

2.4. Extraction of collagen from fish scales

Extraction of collagen from fish scales involves two sequential steps, viz.

Step I: Fish scales were demineralized using EDTA.

Step II: Isolation of collagen by dilute acetic acid treatment.

Both processes were carried out at 4°C to avoid the denaturation of the helical pattern of collagen.

2.5. Demineralization

Fish scales of *LabeoRohita* (Rohu) and *CatlaCatla* were collected from local market and washed thoroughly with distilled water. Next, the scales were washed with a solvent system described elsewhere[37], containing 1 M NaCl, 0.05 M Tris HCl and 20 mM EDTA at pH 7.5 for a

period of 48 h to remove unwanted proteins from the surface. Demineralization of the scales was achieved by treating with 0.5 M EDTA solution for 48 h (pH 7.4). The demineralized fish scale was repeatedly washed with distilled water for three times and used further.

2.6. Isolation of collagen

Demineralized fish scales were treated with 0.5 M acetic acid solution at pH 2.5 over a period of 48 h and the insoluble part of the scales was filtered out. Sodium chloride was added to the filtrate to a final concentration of 5% (w/v) to induce salting out of collagen and kept undisturbed for 24 h at 4°C. The suspension was centrifuged at 10,000 rpm for 30 min and the precipitate was re-solubilized in 0.05 M acetic acid. The salting out and centrifugation steps were repeated thrice for better purification of collagen. The final solution was then dialyzed using a dialysis membrane against 0.005 M acetic acid and distilled water for 24 h each and freeze-dried.

2.7. Preparation of graphene oxide –collagen 3D scaffold

GO solution (2 mg/mL) was prepared with the addition of 100 mg of GO in 50 ml of 0.1 M MES buffer to maintain the pH of the solution at 6.5 and treated with a probe sonicator (125 W Qsonica Sonicators Q125 Sonicator, Qsonica, LLC, Newtown, CT, USA) set at 30% intensity for 30 min in an ice bath. To activate the carboxyl groups of the GO flakes, EDC HCl, and NHS were added into the GO solution (50 mL) at a GO: EDC: NHS molar ratio of 1:2:2[38] and stirred with a magnetic bar for 24 h. About 0.5 g of fish scale type I collagen was dissolved in 50 ml of 1% acetic acid solution and it was added to the EDC/NHS activated GO solution and allowed the reaction to proceed further for another 24 h at room temperature to obtain the final product of collagen functionalized NGO (CFNGO) (covalent interaction between NGO and fish scale

collagen) (Scheme 1). The resultant solution was purified by exhaustive dialysis against double distilled water for 48 h, and lyophilized in the form of sponge.

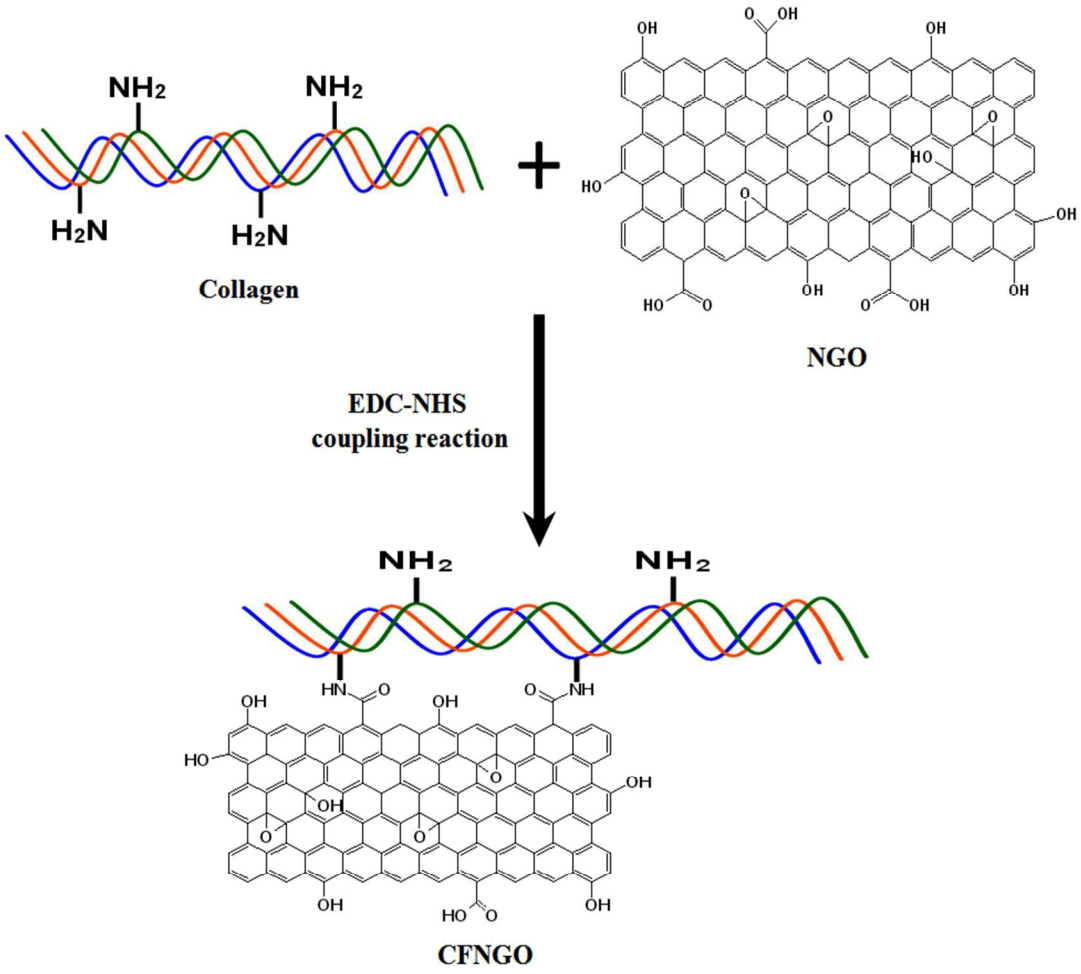

Scheme 1. Covalent amide interaction between NGO and collagen-a representative image

2.8. Preparation of curcumin loaded CFNGO scaffold

Curcumin loaded CFNGO was prepared by a simple, non-covalent interaction method. The loading of curcumin onto CFNGO scaffold was carried out by mixing 10 ml of curcumin solution (60 mg of curcumin) in acetone with 60 ml of a freshly prepared solution of CFNGO

(60 mg of CFNGO scaffold) with constant stirring for 24 h, at room temperature. The suspension was then squeezed through a muslin cloth to remove any precipitate formed during the process and finally the solution was lyophilized (Scheme 2).

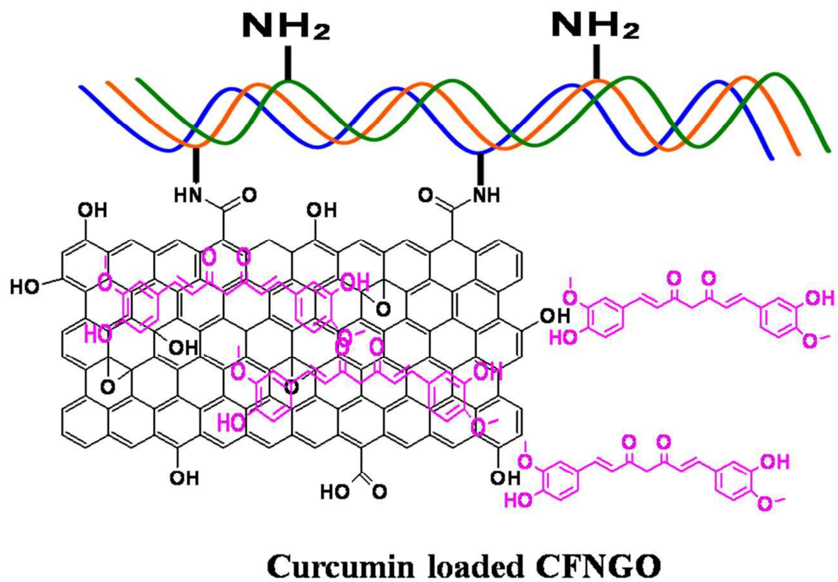

Scheme 2. A representative image of noncovalent interaction (ionic/H-bond and π-π stacking interaction) between curcumin and CFNGO scaffold.

2.9. Dispersion Study

Graphite and GO (single and doubly oxidized) (1 mg/ml) were dispersed in water and sonicated for only 10 min in order to preserve their characteristic layers. All dispersions were left to settle for 24 h at room temperature.

2.10. Morphology of the scaffold

The surface morphology of the collagen and CFNGO scaffolds was assessed using scanning electron microscope (SEM) (ZEISS EVO-MA 10 Scanning Electron Microscope) at a high voltage of 15 kV.

2.11. Transmission electron microscopy (TEM)

The morphology and size of NGO, collagen and CFNGO were examined by using JEOL JEM 2100 HR with EELS transmission electron microscopy (TEM, JEOL, Japan) operated at 200 kV.

2.12. Atomic force microscopic (AFM) analysis

Tapping-mode Atomic force microscopy (AFM) experiments were performed (Innova, Bruker AXS Pte Ltd) to detect the morphology and size of NGO, collagen and CFNGO. To perform the experiment the dilute aqueous dispersion of the samples (10 μL, 0.1 mg mL^{-1}) were casted on a freshly cleaved mica surface and dried in room temperature, the plates were washed again with double distilled water and dried completely at room temperature.

2.13. Dynamic light scattering (DLS)

DLS measurement was performed on a Zetasizer Nano Series (Malvern), it was used to analyze GO hydrodynamic diameters and size distribution.

2.14. Spectroscopic analysis

UV-vis absorption spectra were obtained on a Perkin Elmer Lambda 25 UV-vis spectrophotometer.

2.15. Analysis of functional groups by FT-IR spectroscopy

The analysis of the functional groups present in NGO, collagen and CFNGO were made by a Fourier transform infrared spectrophotometer (Alpha, Bruker, Germany). All spectra were recorded at the resolution of 4 cm^{-1} in the range of 400-4000 cm^{-1}.

2.16. Raman spectroscopy

Raman spectrum of NGO was obtained by use of a back scattering geometry using a micro-Raman setup consisting of a spectrometer (model LabRAM HR, JobinYvon) and a Peltier-cooled charge-coupled device (CCD) detector. An air cooled argon ion laser with a wavelength of 633 nm was used as the excitation light source. Raman spectra of all the samples were recorded at room temperature in the frequency range 0-4000 cm^{-1}.

2.17. X –ray diffraction analysis

The X-ray diffraction of graphite nanopowder, NGO, collagen and CFNGO was performed by a wide angle X-ray scattering diffractometer (Panalytical X-ray Diffractometer, model-X´pert Pro) with Cu-k_α radiation (λ=1.54060Å) in the range of 5-69° (2θ) at 40 KV and 30 mA.

2.18. Analysis of Mechanical properties

Mechanical properties, viz., Young's modulus, tensile strength and the maximum stretching length of the scaffolds were measured using a Universal Testing Machine (LLOYD model no LR10k Plus) at a crosshead speed of 5 mm min^{-1} at 25ºC and at 65% relative humidity. Length and width of the dumbbell shaped test samples were maintained at 20 and 5 mm respectively. All of the mechanical tests were performed with dried samples and were examined in triplicate.

2.19. Thermo gravimetric analysis (TGA)

Thermal decomposition analyses of collagen and CFNGO were carried out under nitrogen flow (40 and 60 ml min^{-1}) with ramp of 20ºC min^{-1} using a TGA Q 50 (V20.6 build 31) instrument.

2.20. Estimation of interacted amine group of collagen in CFNGO by TNBS assay

The analysis of the interacted amine groups was quantified using TNBS assay according to the procedure summarized by Manna et al[38]. In brief, native and interacted (collagen and CFNGO) scaffolds were cut into small pieces of size 4.5 mm. Six milligrams of cut pieces were immersed in a 2 ml of solution consisted of 1 ml of 4% (w/v) di-sodium hydrogen orthophosphate and 1ml of 0.5% (v/v) TNBS, and incubated at 40°C for 2 h. Termination of reaction was done with the addition of 3 ml of 6M (v/v) HCl solution and the incubation was continued at 60°C for 90 min. The absorbance of the resulting solution was measured at 345nm and the interacted amine group was calculated from the difference in the absorbance divided by the absorbance of the native material and then multiplied with 100. The absorbance of the resulting mixture was measured at A_{345} nm using UV-Visible spectrophotometer.

2.21. Swelling ratio test

The swelling ratio test was carried out as follows. A total of 2-5 mg of dry sample was placed in 1.5 ml of physiological saline buffer at 37°C for a period of 72 hours. Upon equilibrium with water, the swelling ratio was calculated according to the following equation:

$$SR\ (\%) = (W_S - W_d / W_d) * 100,$$

Where W_S and W_d are the swollen and dry sample masses, respectively. Swollen samples were paper blotted prior to measurement of W_S.

2.22. Hemolytic assay

Blood compatibility was examined by hemolytic assay. Fresh human blood was used in this study. Blood was collected from the patients followed by ethical clearance and prior informed consent. The sample size was fixed as 12 comprising six male and six female healthy patients. RBC lysis investigates the protein denaturing effect of curcumin loaded CFNGO using a biological material (RBC) as a substrate. Freshly isolated RBCs were incubated in phosphate buffer saline. An irritating substance will cause lysis of the RBCs, leading to the release of hemoglobin in the sample. The cell debris and intact cells were separated by centrifugation and the amount of hemoglobin, which corresponded to the number of cells lysed by the curcumin loaded CFNGO, was assayed by spectrophotometry. At first, different volume of samples in tubes (10, 20, 30, 50, 75, 100 µl) were taken and made up to 950 µl with PBS, followed by the addition and mixing of 50 µl of RBC sample. The samples were incubated in the dark for 10 minutes and then centrifuged for 10 minutes at 6,000 RPM. The OD value of the supernatant was measured at 540 nm using a spectrophotometer. The obtained results were compared with the positive control (50 µl RBC + 950 µl H_2O) and the negative control (50 µl RBC + 950 µl PBS). Each concentration was evaluated in triplicate. The percentage of lysis calculated by the formula; % lysis = (OD of sample – OD of positive control) X 100 / (OD of negative control – OD of positive control)[38]

2.23. Cell culturing and maintenance

NIH 3T3 embryonic mouse fibroblast cells, procured from NCCS, Pune, India, were used for the present study. The cultures were maintained in DMEM supplemented with 10%Fetal Bovine Serum (FBS), 200 mM Glutamine, 2 mg ml^{-1}sodium bicarbonate and 1× antibiotic and

antimycotic solution. Periodically the medium was replaced. The cells were cultured in tissue culture flasks and incubated at 37°C in a humidified atmosphere of 5% CO_2. Trypsin at 0.05% was used to detach the cells.

2.24. Cell adherence and proliferation

NIH 3T3 cell adherence and proliferation assessment of collagen and curcumin loaded CFNGO was carried out with collagen and curcumin loaded CFNGO pre-coated culture plates. In brief, 2 ml of collagen and the prepared curcumin loaded CFNGO solution were added to each well of twelve-well culture plates and subjected to air drying at 40°C. The control wells were not coated with anything. The dried plates were then surface sterilized with 70% alcohol for 30 min followed by UV sterilized for 1h. Next, the plates were washed with sterile PBS for 1 h. A cell density of 3×10^4 cells per well was seeded and incubated with the growth medium for the period of 12, 24 and 48 hours, and the observations on cell viability, adherence and proliferation were made as described below. The cell adherence and proliferation of fibroblast cells were visualized and quantified by live cell tracker assay and MTT assay methods. With respect to the cell tracker assay, after scheduled time intervals (12, 24, 48 hours), the medium was removed and washed with PBS. Calcein AM solution (4 mM; 500ml) was added and the sample was incubated for 30 min. The plates were then washed with PBS and viewed at fluorescence excitation and emission wavelengths of 495/515 nm, respectively, using a fluorescence microscope with a blue filter (Euromex, Holland.). With regard to the MTT assay, the culture medium of each well was replaced with MTT (5 mg ml^{-1}dilutedin serum-free medium) and incubated at 37°C for 4 hours. After the removal of MTT solution, dimethyl sulfoxide was added and the medium was left at room temperature for two minutes and the absorbance was recorded at 570 nm using a plate reader (Epoch, BIOTEK).

2.25. Cell migration assay

A cell migration assay was performed according to the method summarized[39]. NIH 3T3 cells were harvested by trypsinization and loaded in a 48-well plate at a concentration of 5×10^4 cells per well, and allowed to form a uniform monolayer. Followed by attaining 80 to 85% cell confluence, a scratch was introduced using a sterile 200 ml tip. The plates were then washed with PBS to remove the dead cells and supplemented with DMEM medium containing collagen and CFNGO. Wells filled with the medium alone served as a control. Migration of cells and the reduction in empty space were measured at 0, 12and 24 hours of incubation using Image J software.

2.26. Cell morphology of NIH 3T3 cells in CFNGO scaffold

Curcumin loaded CFNGO scaffold (2×2×1 cm) was placed individually in 6 well culture plates (Tarson, India) and ETO (Ethylene Oxide) sterilized. Culture media was added to the scaffold for overnight. NIH 3T3 fibroblast cells was seeded on to the scaffold at a density of 5×10^4 cells and incubated in an atmosphere of 5% CO_2 at 37°C. The medium was changed every 24 h. Morphology of the cells were examined after 12 days according to the following procedure. The cells-scaffold construct was fixed in 2.5% glutaraldehyde and dehydrated through graded ethanol series. The dried cells-scaffold was coated with gold and examined under SEM (ZEISS EVO-MA 10 Scanning Electron Microscope).

2.27. *In vitro* curcumin Release

A known amount of curcumin loaded CFNGO scaffold (70 mg) was immersed in 3 ml of phosphate buffer solution, pH 7.4 at 37°C, followed by the transfer into 7 centrifuge tubes and was kept in a shaker. Free curcumin was not soluble in water; therefore, at predetermined time

intervals, the solution was centrifuged at 5000 RPM for 9 min to separate the released curcumin from the CFNGO scaffold. The released curcumin was redissolved in 3 ml of ethanol and determined its concentration by UV-Vis spectrometer at 425 nm. The concentration of releasing curcumin was then calculated using a standard curve of curcumin in ethanol. The percentage of curcumin released was determined from the following equation: curcumin release (%) = 100 × curcumin released on time (t) /total curcumin loaded in CFNGO scaffold.

2.28. Evaluation of antimicrobial activity

The antimicrobial activity of the prepared curcumin loaded/not loaded CFNGO scaffold was tested by the disc diffusion method against gram-negative bacteria namely *P. aeruginosa* and gram-positive bacteria namely *S. aureus*. The scaffolds were cut into a disc shape with 5 mm diameter followed by sterilization under UV light for 10 min and placed on agar plates with cultures. The plates were incubated for 24 h at 37°C in an incubator and the zone of inhibition was then calculated. The zone of inhibition was not observed for native CFNGO scaffold (not loaded with curcumin). This experiment was performed in triplicate with each organism and an average diameter of zone of inhibition was noted.

2.29. Evaluation of wound healing efficacy of curcumin loaded CFNGO scaffold

In order to assess the efficacy of curcumin loaded CFNGO scaffold as wound cover, animal model study was taken up with prior approval from the ethical committee; with vide approval No.466/01a/CPCSEA for open wound model studies. Male Albino rats (Wistar strain) of weight ranging over 125–150 g were used for the present study. They were housed individually in standardized environmental conditions, feed with pellet rodent diet and water ad libitum. Animals were randomly grouped into three groups with six animals per group. Group-1

(Control-wound covered with cotton soaked in Phosphate buffered saline); Group-II (Wound covered with scaffold prepared from collagen alone); Group-III (Wound covered with scaffold of curcumin loaded CFNGO scaffold). An incision of 4 cm $(2\ cm)^2$ was created on the dorsal part of all the rats with the help of scissors and surgical blade and the wound area was sterilized with surgical spirit. Respective dressing scaffolds were applied to animals and closed with gauze. All the rats were received regular dressing changes at every alternative day.

2.30. Rate of wound contraction area

Wound contraction was measured as a percentage reduction in wound size at every 4 day interval and photographed. Progressive decrease in the wound size was monitored periodically by tracing the boundary and the area was accessed graphically.

The biodegradability of the CFNGO and native collagen scaffold summarized in detail in supplementary file S1.

3. RESULTS AND DISCUSSIONS

It has been observed that graphite and NGO (single and double oxidized) look differently because of their distinct structural and physicochemical properties. Black particles are visible in the graphite dispersion after sonication for 0.5 h. Most of graphite particles precipitated after 0.5 h of graphite dispersion. The singly oxidized NGO dispersion is blackish yellow in color. Some small NGO particles can also be identified in the NGO dispersion. Significant portion of NGO particles precipitated after the NGO dispersion was idle for 2 h. However, clear and homogeneous yellow colored dispersion is observed for doubly oxidized NGO. The NGO dispersion was stable after standing still for several days, could be due to the large amount of

hydrophilic functional groups, such as carboxyl, hydroxyl, and epoxy groups, on NGO nanosheets[40].

Morphology of the scaffold

The surface morphology of collagen and CFNGO scaffolds is shown in Figure 1a. Compared to native collagen scaffold, CFNGO scaffold is highly porous (the porosity of CFNGO was observed at around 10-20μm) and the pore structures of the membranes were well-distributed and interconnected. The conjugation of NGO with collagen increases the scaffold pore size in CFNGO, as determined by SEM images. It is obvious that most of the volume of the membranes were taken up by the interconnecting pore space. The high porosity suggests the suitability of this scaffold for biomedical applications, including serving as absorption sponges and matrices for cell proliferation.

Transmission electron microscopy (TEM)

TEM images of collagen show the existence of collagen fiber, whereas NGO shows that it is fully exfoliated into individual sheets (Figure 1b). In CFNGO image, NGO nano sheet is observed randomly distributed inside the collagen fiber, and substantiates the interaction between amine group of collagen and carboxylic group of NGO. As a result, all the randomly distributed collagen fibers (as shown in Figure 1b) came close to each other which could be the reason for high mechanical strength of the CFNGO scaffold. The following scheme 3 shows how collagen fiber and NGO is co-existed in CFNGO scaffold, the white arrow indicates the presence of NGO and black arrow indicates the collagen fiber existence inside the tem image of CGNGO.

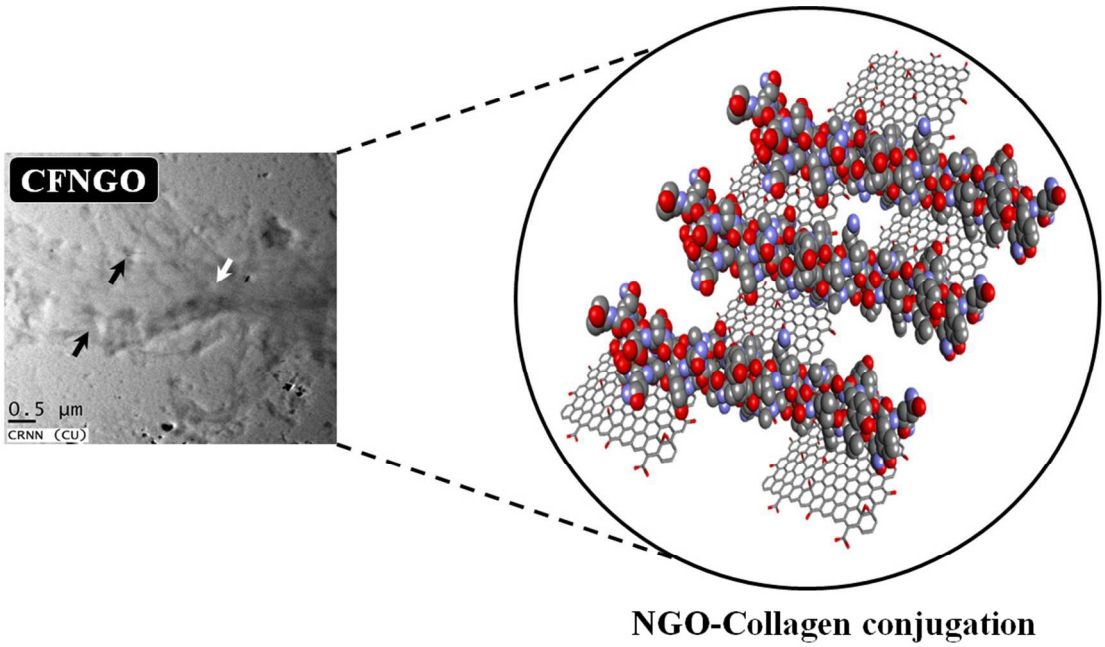

Scheme 3. The scheme represents the pattern of NGO and collagen conjugation.

Atomic force microscopic analysis (AFM)

The AFM images (Figure 1c), show 2D surface morphology of collagen fiber and ultrathin (1.5 nm thick) NGO sheets which is typical for a one-atom-thick GO nano-layer[40, 41]. Figure 1c present the representative AFM image of the CFNGO scaffold and it confirms the presence of uniform layers of NGO and collagen fibers together, suggesting the successful interaction between NGO and collagen.

Size distribution by dynamic light scattering (DLS)

Figure 1d depicts the hydrodynamic size of the prepared doubly oxidized NGO nano sheet in the range between 60- 600 nm with major peak in 220-350 nm range. All results reflect the average of three measurements and the difference between each measurement was < 5%.

Spectroscopic analysis

In the UV-vis spectrum (Figure 2a), fish scale collagen showed one peak at 213 nm due to the presence of amide linkage and one small hump is observed at around 280 nm due to the presence of very small amount of aromatic residues (phenylalanine and tyrosine)[42, 43]. NGO showed a characteristic peak at 231 nm (corresponding to π–π* transitions of C=C bonds) and a shoulder at 300 nm (due to n–π* transitions of –COOH groups)[44]. And in CFNGO spectrum one peak observed at 216 nm which could be due to the presence of C=O, –COOH and $–CONH_2$ groups in CFNGO and one peak at 300 nm as observed in NGO spectrum has disappeared due to the interaction of –COOH group of NGO and free primary amine group of collagen.

FT-IR assessment

FT-IR experiments were carried out to investigate the covalent amide ($–CONH_2$) interaction between NGO and collagen. Figure 2b illustrates FT-IR spectrum of collagen, NGO and CFNGO scaffolds. The FT-IR spectrum of NGO and collagen were similar to those previously presented in literature[45-47]. In the collagen spectrum the peak at 3282 cm^{-1} is attributed to $–NH_2$ stretching vibration and at 3078 cm^{-1} for fermi resonance overtone of 1539 cm^{-1} band, furthermore 2927 cm^{-1} for C–H stretching. The bands at 1626, 1539 and 1390 cm^{-1} correspond to C=O stretching (Amide I), N–H bending (Amide II) and C–N stretching (Amide III) of amide ($–CONH_2$) linkages in collagen protein. The peak at 1236 cm^{-1} is due to the C–N stretching of amine[47].

In the NGO spectrum, the peaks appear at 3384 cm^{-1}, 1700 cm^{-1}, 1640 cm^{-1}, 1035 cm^{-1} are assigned to –OH stretching vibration, C=O stretching vibration of the carboxylic group, C=C stretching mode of the sp^2 network and C–O stretching vibration respectively[45], demonstrating the presence of –COOH and –OH groups in the NGO.

By comparing the spectra of CFNGO scaffold, it has been found that there are no additional peaks excluding the specific bands of collagen and NGO but with a greater intensity and accordingly ascribed to the EDC-NHS coupling interaction between NGO and collagen through the $–CONH_2$ (amide) linkage between –COOH group of NGO and free primary $–NH_2$ group of collagen and result in an enhanced mechanical response.

Raman spectroscopy

Raman spectroscopy gives useful information related to the structural properties of NGO. A typical Raman spectra of the sample was shown in figure 2c. Raman spectra of NGO showed three distinctive signals: A band close to 1590 cm^{-1} (G band), another one around 1330 cm^{-1} (D band) and 2D band in the region of 2740 cm^{-1}.[48, 49]The G band originates from in-plane vibration of sp^2 carbon atoms of the graphite lattice[50, 51]. D band is due to the out-of-plane breathing mode of the sp^2 atoms, it reveals the presence of certain defects, whereas 2D is the second order of this vibrational mode[44, 52]. These observations confirmed the layer separation of the NGO structure and the corresponding 2D band indicates considerable defects in the graphene sheet, produced by oxidation[52].

X –ray diffraction analysis

Figure 2d depicts the X-ray diffractograms of graphite nanopowder, NGO, collagen and CFNGO scaffolds. It has been observed that the most intense peak for graphite is at $2\theta = 26.5°$ and d spacing is 3.3Å, whereas NGO spectrum exhibits a characteristic peak at $2\theta = 10.4°$ with the d spacing of 8.5Å which is within the range of values that has been previously reported[53]. The above results indicate that the interlayer distance for NGO is significantly larger than that of the graphite. These observations suggested that the successful oxidation of the graphite to NGO

intended the oxygenated functional groups on carbon sheets which ultimately increase the interlayer space of NGO. The oxidation of graphite to NGO has already been confirmed by ATR-FTIR spectra as described earlier.

The characteristic peak of collagen appeared at the positions 2θ= 22° with average intermolecular distance of 3.9Å, this broad peak indicates a typical diffraction pattern for collagen.

The diffraction spectrum of the CFNGO scaffold displayed broad spectrum at 2θ = 23° indicating its amorphous nature and intermolecular distance observed 3.8Å which is less than that of the NGO (8.5Å), could be due to the aggregation of NGO with collagen.

Mechanical property

The mechanical property of CFNGO scaffold showed significant enhancement compared to the collagen scaffold alone. The tensile strength of CFNGO scaffold is 3.19 MPa, where the tensile strength of native collagen scaffold is only 0.09 MPa. Nearly threefold increment of the tensile strength has been observed for CFNGO scaffold compared to the native collagen scaffold. The strain at maximum load for CFNGO scaffold is observed much higher than that of the native collagen may be due to the covalent interaction between NGO and collagen, which has already been confirmed by ATR-FTIR analysis. The ultimate tensile strength (MPa), strain at maximum load and Young's modulus (MPa) of native collagen and CFNGO scaffold are summarized in Table 1. All results reflect the average of three measurements, and the difference between each measurement was < 5%.

Thermo gravimetric analysis (TGA)

Thermal stability of scaffolds is evaluated with TGA. Major thermal decomposition of native collagen occurs in the temperature between 300-400°C (Figure 2e) and the corresponding thermal degradation values are listed in Table 2. The major decomposition of the CFNGO scaffold initiated after 350°C, (at 400°C 41% weight loss is observed and 50% weight loss is at 800°C) and only 9% of weight loss is observed at 800°C suggested that CFNGO scaffold is much more thermally stable compared to native collagen scaffold due to the covalent interaction between NGO and collagen. The thermal stability also influences on the durability of the scaffolds.

The percentage of the interacted amine group is observed as 47% for CFNGO scaffold.

Hemolysis

The hemolysis assay is a significant index of the material for the application in the biomedical field because the material is usually exposed to blood environment and damaged the erythrocytes in a certain extent. In the present study, the assay is carried out to evaluate the blood compatibility of curcumin loaded CFNGO scaffold. As shown in Figure 3a, no damage on the erythrocytes by CFNGO scaffold infers the hemocompatibility of the prepared scaffold. All the results reflect the average of three measurements, and the difference between each measurement was < 5%.

Water holding capacity

The water holding capacity of the scaffold plays an important role in tissue engineering. The swelling ratio of native collagen scaffold is 1925% (±12.1) and for CFNGO scaffold it is 3579% (±10.3). It has been understood that water holding capability of CFNGO scaffold is much higher than that of the native collagen scaffold due to the incorporation of NGO. The swelling

ratio of the scaffold strongly depends on the hydrophilic nature and microstructure of the scaffold. Since collagen (presence of $–NH_2$ and –COOH group) and NGO (due to the presence of numerous –COOH and –OH groups) are both hydrophilic materials, CFNGO scaffold has higher water retention capability with appreciable mechanical property. The poor mechanical properties of collagen led to the collapse of the porous structure when it is taken out from PBS solution. Contrarily, NGO possesses higher mechanical stability which is helpful for the retention of the scaffold original porous structure. All the obtained results are the average of three measurements, and the difference between each measurement was < 5%.

Cell adhesion and proliferation profile of CFNGO scaffold

It is very essential to evaluate the cytotoxicity of the prepared curcumin loaded CFNGO scaffold, when the scaffold is used in biological and biomedical applications, such as drug delivery and gene transfection. In the present study, the cell adherence and cell proliferation potentials of the curcumin loaded CFNGO scaffold are assessed using NIH3T3 cells. Figure 3b shows the fluorescence images of the cells observed at different time intervals. When cells are stained with a calcein fluorescent probe, a cell-permeant dye, in live cells the non-fluorescent calcein AM converted to a green-fluorescent calcein after acetoxymethyl ester hydrolysis by intracellular esterases. In the present study, no significant difference is seen in fluorescence intensity in the curcumin loaded CFNGO scaffold-treated cells compared to the control. Furthermore, no morphological changes are observed in the curcumin loaded CFNGO scaffold-treated cells. Results on cell viability and quantification suggested that more than 90% of the cells are viable and incorporation of curcumin and NGO into collagen does not exert adverse effects on cell viability (Figure 3c). It has already been reported that the cytotoxicity of NGO is dose-dependent and a small quantity of NGO does not negatively affect the viability of cell[54-56].

The improved hydrophilicity due to the hydrophilic groups of NGO and collagen provides higher cell adhesion on collagen and curcumin loaded CFNGO scaffold than control since cells adhere, spread and grow more easily on moderately hydrophilic surfaces than on hydrophobic ones[57]. It is considered that relatively higher hydrophilicity of collagen and curcumin loaded CFNGO scaffold promote the adhesion of cells.

***In vitro* cell migration assay**

Results on cell migration studies of the curcumin loaded CFNGO scaffold using NIH 3T3 cells suggest that compared to the control (untreated) curcumin loaded CFNGO scaffold-treated cells migrate at the fastest rate and more than 90% of the scratch area is covered by the cells within 24 hours (Figure 3d) similar to the collagen scaffold-treated cells. The observations suggest that the curcumin loaded CFNGO scaffold influences cell migration, and this property adds value to the material for its application in wound healing studies.

Cell morphology of NIH 3T3 cells in CFNGO scaffold

The SEM images of the cell seeded curcumin loaded CFNGO scaffold displayed in Figure 3e demonstrated that after being cultured for prolonged time (12 days), fibroblasts were detected in the scaffolds (curcumin loaded CFNGO) with typical spindle shaped morphology and suggests that the cells were infiltrated into the scaffolds and proliferated there.

The release of curcumin from CFNGO scaffold is conducted in phosphate buffer solution to evaluate its sustained delivery. The average concentration of curcumin release from curcumin loaded CFNGO scaffold is approximately 12.1, 14.5, 18.9, 20.6, 27.7, 36.1, 52.7, 78.7 and 82.5% in the respective duration of 1, 3, 6, 9, 12, 24, 48, 72 and 96 h. Comparing all of these results, it is confirmed that the curcumin loaded CFNGO scaffold prepared in the present study has a better

sustained release property. The material with the above said property will be very helpful as a wound dressing material because the curcumin will release on the wound site at a slower rate and this will restrict the bacterial growth for a prolonged time, leading to quick subsequent wound healing.

The antibacterial activity of curcumin loaded CFNGO scaffold are obtained as 15 (±3) and 16 (±2) mm against gram-negative *P. aeruginosa* and gram-positive bacteria *S. aureus.* Due to this antibacterial property, it can be applied as an efficient wound healing material because the inherent antimicrobial property of the material will not allow the microbial growth on the wound site, leading to quick healing of the wound. Nguyen et al reported similar kind of observation for the preparation of curcumin loaded chitosan/gelatin composite sponge for wound healing application[58].

The curcumin loaded CFNGO scaffold also subjected to test as a wound dressing material (open wound) using animal models (Wistar strain). Figure 4 illustrates the progressive wound closure of three different experimental groups. The control group (Group-I) took more than 20 days for complete closure, whereas, complete wound closure was evidenced within 16 days for Group-II (collagen alone) and 12 days for Group-III (curcumin loaded CFNGO scaffold) animals. Similarly, wound contraction measurements (Table 3) also showed accelerated wound closure in both Group-II and Group-III animals compared to Group-I. The results discussed over here were the representative results obtained for curcumin loaded CFNGO scaffold.

4. Conclusions

The current scenario on biomaterials research suggested that the demand on new materials with advanced functional properties to meet the challenges. Though, biocompatibility and biodegradability properties have been incorporated to the material via functionalization and modification procedures, materials for drug delivery studies lacking the property of simultaneous release of both hydrophobic and hydrophilic drugs. Since, incorporation of graphene oxide demonstrates appreciable role in imparting strength to the materials, cross-linking of nano graphene oxide with collagen may found suitable for the delivery of drugs, growth factors or cells as a unique delivery system irrespective of the nature of the delivery molecules. Hence, an attempt was made in the present study to reinforce nano graphene oxide to fish scale collagen via EDC-NHS coupling methods, and curcumin drug was incorporated into CFNGO by non covalent interaction. The resulting curcumin loaded CFNGO establishes appreciable mechanical strength (when 2% of NGO was mixed with 1% of collagen), cell adherence and proliferation, biocompatibility, etc. The antimicrobial study reveals the curcumin loaded CFNGO scaffold has appreciable antibacterial activity. Animal model wound healing studies further explores, curcumin loaded CFNGO scaffold acts as a wound dressing material. The supplementary file proves that the obtained material is enzymatically degradable at physiological condition. The presence of various functional groups in NGO-collagen scaffold suggested the possibility of use of the scaffolds for multidrug delivery. A study on the process of delivery of multidrug using NGO-Collagen scaffold has been initiated and the observations will soon be in the public domain.

Acknowledgements

One of The authors Dr. Tapas Mitra acknowledges UGC, New Delhi for financial assistance provided in the form of Dr. D. S. Kothari Post-Doctoral Fellowship. All authors

thanks to Dr. Achintya Singha, Department of Physics, Bose Institute, 93/1, Acharya Prafulla Chandra Road, Kolkata 700009, India for his assistance to perform Raman Spectroscopic analysis. Authors are acknowledging Mr. Sourav Chakraborty, Calcutta University – DBT Interdisciplinary Program in Life Science (DBT-IPLS), 35 Ballygunge Circular Road Kolkata-700019 to perform AFM analysis. Authors are also acknowledge Miss Urmila Goswami, CRNN, University of Calcutta, JD-2, Salt Lake City, Kolkata 700098, West Bengal, INDIA for her help to take TEM images of the samples.

References

1. C. P. Barnes, S. A. Sell, E. D. Boland, D. G. Simpson and G. L. Bowlin, *Advanced drug delivery reviews*, 2007, **59**, 1413-1433.

2. M. F. Desimone, C. Helary, G. Mosser, M.-M. Giraud-Guille, J. Livage and T. Coradin, *Journal of Materials Chemistry*, 2010, **20**, 666-668.

3. Z. Xia, X. Yu, X. Jiang, H. D. Brody, D. W. Rowe and M. Wei, *Acta biomaterialia*, 2013, **9**, 7308-7319.

4. B. Balakrishnan, M. Mohanty, P. R. Umashankar and A. Jayakrishnan, *Biomaterials*, 2005, **26**, 6335-6342.

5. M. Ogawa, M. W. Moody, R. J. Portier, J. Bell, M. A. Schexnayder and J. N. Losso, *Journal of Agricultural and food Chemistry*, 2003, **51**, 8088-8092.

6. A. Jongjareonrak, S. Benjakul, W. Visessanguan, T. Nagai and M. Tanaka, *Food Chemistry*, 2005, **93**, 475-484.

7. G. Bilgen, G. Oktay, Z. TokgoZ, G. Guner and S. Yalcin, *Turkish Journal of Veterinary and Animal Sciences*, 1999, **23**, 483-488.

8. T. Nagai, Y. Araki and N. Suzuki, *Food chemistry*, 2002, **78**, 173-177.

9. T. Nagai, M. Izumi and M. Ishii, *International journal of food science & technology*, 2004, **39**, 239-244.

10. T. Nagai and N. Suzuki, *Food Chemistry*, 2000, **68**, 277-281.

11. D. Swatschek, W. Schatton, J. Kellermann, W. E. G. Muller and J. Kreuter, *European Journal of Pharmaceutics and Biopharmaceutics*, 2002, **53**, 107-113.

12. S. Park and R. S. Ruoff, *Nature nanotechnology*, 2009, **4**, 217-224.

13. D. R. Dreyer, S. Park, C. W. Bielawski and R. S. Ruoff, *Chemical Society Reviews*, 2010, **39**, 228-240.

14. Y. Zhu, S. Murali, W. Cai, X. Li, J. W. Suk, J. R. Potts and R. S. Ruoff, *Advanced materials*, 2010, **22**, 3906-3924.

15. M. Tang, Q. Song, N. Li, Z. Jiang, R. Huang and G. Cheng, *Biomaterials*, 2013, **34**, 6402-6411.

16. J. Hong, N. J. Shah, A. C. Drake, P. C. DeMuth, J. B. Lee, J. Chen and P. T. Hammond, *Acs Nano*, 2011, **6**, 81-88.

17. L. Zhang, J. Xia, Q. Zhao, L. Liu and Z. Zhang, *Small*, 2010, **6**, 537-544.

18. G. Y. Chen, D.-P. Pang, S. M. Hwang, H. Y. Tuan and Y. C. Hu, *Biomaterials*, 2012, **33**, 418-427.

19. W. C. Lee, C. H. Y. X. Lim, H. Shi, L. A. L. Tang, Y. Wang, C. T. Lim and K. P. Loh, *ACS nano*, 2011, **5**, 7334-7341.

20. T. R. Nayak, H. Andersen, V. S. Makam, C. Khaw, S. Bae, X. Xu, P.-L. R. Ee, J.-H. Ahn, B. H. Hong and G. Pastorin, *ACS nano*, 2011, **5**, 4670-4678.

21. H. Bao, Y. Pan, Y. Ping, N. G. Sahoo, T. Wu, L. Li, J. Li and L. H. Gan, *Small*, 2011, **7**, 1569-1578.

22. X. Sun, Z. Liu, K. Welsher, J. T. Robinson, A. Goodwin, S. Zaric and H. Dai, *Nano research*, 2008, **1**, 203-212.

23. K. Yang, J. Wan, S. Zhang, Y. Zhang, S.-T. Lee and Z. Liu, *ACS nano*, 2011, **5**, 516-522.

24. W.-G. La, S. Park, H.-H. Yoon, G.-J. Jeong, T.-J. Lee, S. H. Bhang, J. Y. Han, K. Char and B.-S. Kim, *Small*, 2013, **9**, 4051-4060.

25. X. Shi, H. Chang, S. Chen, C. Lai, A. Khademhosseini and H. Wu, *Advanced Functional Materials*, 2012, **22**, 751-759.

26. C. Cha, S. R. Shin, N. Annabi, M. R. Dokmeci and A. Khademhosseini, *ACS nano*, 2013, **7**, 2891-2897.

27. K. P. Loh, Q. Bao, G. Eda and M. Chhowalla, *Nature chemistry*, 2010, **2**, 1015-1024.

28. E.-M. Strasser, B. Wessner, N. Manhart and E. Roth, *Biochemical pharmacology*, 2005, **70**, 552-559.

29. S. Han and Y. Yang, *Dyes and pigments*, 2005, **64**, 157-161.

30. O. Vajragupta, P. Boonchoong, G. M. Morris and A. J. Olson, *Bioorganic & medicinal chemistry letters*, 2005, **15**, 3364-3368.

31. B. B. Aggarwal, A. Kumar and A. C. Bharti, *Anticancer res*, 2003, **23**, 363-398.

32. S.-Y. Park, H.-S. Kim, E.-K. Cho, B.-Y. Kwon, S. Phark, K.-W. Hwang and D. Sul, *Food and Chemical Toxicology*, 2008, **46**, 2881-2887.

33. M. Panchatcharam, S. Miriyala, V. S. Gayathri and L. Suguna, *Molecular and cellular biochemistry*, 2006, **290**, 87-96.

34. S. Bisht and A. Maitra, *Current drug discovery technologies*, 2009, **6**, 192-199.

35. D. Gopinath, M. R. Ahmed, K. Gomathi, K. Chitra, P. K. Sehgal and R. Jayakumar, *Biomaterials*, 2004, **25**, 1911-1917.

36. W. S. Hummers Jr and R. E. Offeman, *Journal of the American Chemical Society*, 1958, **80**, 1339-1339.

37. F. Pati, B. Adhikari and S. Dhara, *Bioresource Technology*, 2010, **101**, 3737-3742.

38. P. J. Manna, T. Mitra, N. Pramanik, V. Kavitha, A. Gnanamani and P. P. Kundu, *International journal of biological macromolecules*, 2015, **75**, 437-446.

39. C.-C. Liang, A. Y. Park and J.-L. Guan, *Nature protocols*, 2007, **2**, 329-333.

40. S. Stankovich, D. A. Dikin, R. D. Piner, K. A. Kohlhaas, A. Kleinhammes, Y. Jia, Y. Wu, S. T. Nguyen and R. S. Ruoff, *Carbon*, 2007, **45**, 1558-1565.

41. H. C. Schniepp, J.-L. Li, M. J. McAllister, H. Sai, M. Herrera-Alonso, D. H. Adamson, R. K. Prud'homme, R. Car, D. A. Saville and I. A. Aksay, *The Journal of Physical Chemistry B*, 2006, **110**, 8535-8539.

42. S. Yunoki, T. Suzuki and M. Takai, *Journal of bioscience and bioengineering*, 2003, **96**, 575-577.

43. P. Bama, M. Vijayalakshimi, R. Jayasimman, P. T. Kalaichelvan, M. Deccaraman and S. Sankaranarayanan, *International Journal of Pharmacy and Pharmaceutical Science*, 2010, **2**, 133-137.

44. J. I. Paredes, S. Villar-Rodil, A. Martinez-Alonso and J. M. D. Tascon, *Langmuir*, 2008, **24**, 10560-10564.

45. L. Liu, C. Li, C. Bao, Q. Jia, P. Xiao, X. Liu and Q. Zhang, *Talanta*, 2012, **93**, 350-357.

46. V. K. Malesu, D. Sahoo and P. L. Nayak, *International Journal of Applied Biology and Pharmaceutical Technology*, 2011, **2**, 402-411.

47. T. Mitra, G. Sailakshmi and A. Gnanamani, *Journal of Chemical Sciences*, 2014, **126**, 127-140.

48. S. Wakeland, R. Martinez, J. K. Grey and C. C. Luhrs, *Carbon*, 2010, **48**, 3463-3470.

49. S. Park, J. An, R. D. Piner, I. Jung, D. Yang, A. Velamakanni, S. T. Nguyen and R. S. Ruoff, *Chemistry of Materials*, 2008, **20**, 6592-6594.

50. K. N. Kudin, B. Ozbas, H. C. Schniepp, R. K. Prud'Homme, I. A. Aksay and R. Car, *Nano letters*, 2008, **8**, 36-41.

51. D. Yang, A. Velamakanni, G. l. Bozoklu, S. Park, M. Stoller, R. D. Piner, S. Stankovich, I. Jung, D. A. Field and C. A. Ventrice, *Carbon*, 2009, **47**, 145-152.

52. T. V. Cuong, V. H. Pham, Q. T. Tran, S. H. Hahn, J. S. Chung, E. W. Shin and E. J. Kim, *Materials letters*, 2010, **64**, 399-401.

53. J. Wang, X. Wang, C. Xu, M. Zhang and X. Shang, *Polymer International*, 2011, **60**, 816-822.

54. K. Wang, J. Ruan, H. Song, J. Zhang, Y. Wo, S. Guo and D. Cui, *Nanoscale Res Lett*, 2011, **6**, 1-8.

55. K.-H. Liao, Y.-S. Lin, C. W. Macosko and C. L. Haynes, *ACS applied materials & interfaces*, 2011, **3**, 2607-2615.

56. E. L. K. Chng and M. Pumera, *Chemistry-A European Journal*, 2013, **19**, 8227-8235.

57. Y. Arima and H. Iwata, *Biomaterials*, 2007, **28**, 3074-3082.

58. V. C. Nguyen, V. B. Nguyen and M.-F. Hsieh, *International Journal of Polymer Science*, 2013, **2013**.

Figure captions

Figure. 1 (a). SEM Micrographs of native collagen and collagen functionalized NGO (CFNGO). **(b)** Transmission electron microscopic (TEM) images of collagen, nano graphene oxide (NGO) and collagen functionalized NGO (CFNGO). (Black arrow indicates the existence of NGO and white arrow indicates the collagen fiber). **(c)** Atomic force microscopic (AFM) images of collagen, nano graphene

oxide (NGO) and collagen functionalized NGO (CFNGO). **(d)** Dynamic light scattering (DLS) based size distribution of nano graphene oxide (NGO).

Figure. 2 (a). UV-Visible absorption spectra of collagen, nano graphene oxide (NGO) and collagen functionalized NGO (CFNGO). **(b)** FT-IR spectra of collagen, nano graphene oxide (NGO) and collagen functionalized NGO (CFNGO) scaffolds. **(c)** Raman spectrum of nano graphene oxide (NGO). **(d)** XRD patterns of (A) graphite powder, (B) nano graphene oxide (NGO), (C) Collagen and (D) collagen functionalized NGO (CFNGO). **(e)** Thermo gravimetric analysis (TGA) of native collagen and collagen functionalized NGO (CFNGO) scaffolds.

Figure. 3 (a). Blood compatibility studies of curcumin loaded CFNGO where 1-6. 10, 20, 30, 50, 75 and 100 µl of curcumin loaded CFNGO sample make up to 950 µl with PBS and then 50 µl of RBC sample was added and mix. 7. Positive control (50 µl RBC + 950 µl H_2O) 8. Negative control (50 µl RBC + 950 µl PBS). **(b)** *In vitro* fluorescence images of NIH 3T3 fibroblast cells on adherence and proliferation on the surface of curcumin loaded CFNGO scaffold in comparison with native collagen and control, at various time intervals of 12, 24 and 48 h. A blue filter was used for fluorescence excitation and emission. The scale bar measures 10 mm. **(c)** Cell viability assessment based on MTT quantification of NIH 3T3 cell population upon being exposed to the curcumin loaded CFNGO in comparison with native collagen and control (all the values are the mean SD of triplicates) under *in vitro* conditions. **(d)** Influence of the curcumin loaded CFNGO scaffold on the migration of fibroblast cells (NIH 3T3) assessed from a scratch assay (*in vitro* conditions). Image J analysis was used to measure the space covered by the

migrated cells at different incubation periods 0, 12 and 24 h. The scale bar measures 10 mm. **(e)** Attachment of fibroblast cells on the curcumin loaded CFNGO scaffold (white arrow indicates the adhered cells on the Scaffold).

Figure. 4. Open wound closer upon treatment with curcumin loaded CFNGO scaffold.

Table 1. Assessment of mechanical properties of native collagen and CFNGO scaffold.

SampleName	Strain at maximum load (%)	Tensile strength (MPa)	Young's Modulus (MPa)
Collagen scaffold	6.58 (±0.5)	0.09 (±0.004)	1.36 (±0.4)
CFNGO scaffold	23.73 (±1.2)	3.19 (±0.5)	25.85 (±1.76)

Table 2. Thermal analysis of native collagen and CFNGO scaffold under N_2 air atmosphere.

Temperature (ºC)	% of weight loss (heating rate 20°C/min)	
	Native Collagen scaffold	CFNGO scaffold
100	13	11
200	15	15
300	26	23
400	62	41
500	70	45
600	74	47
700	77	49
800	80	51

Table 3. Wound contraction measurements in experimental groups of animals

Days	Control (Group-I)		Native collagen (Group - II)		Curcumin loaded CFNGO (Group -III)	
	Wound area (mm^2)*	% of wound contraction*	Wound area (mm^2)*	% of wound contraction*	Wound area (mm^2)*	% of wound contraction*
0^{th}	333.3±42.5	0	358.5±62	0	368.67±48.5	0
4^{th}	250 ±37	10.8±11.28	301.17±68	18.3±16.18	329.5 ±68.5	21.71±20.86
8^{th}	145.83±44.5	55.61±17.39	103.67±31.5	70.28±16.47	100.33 ±90	74.19±26.95
12^{th}	33.5 ±11.5	89.99 ±2.29	12.17 ±5.9	96.57 ±1.88	41.67 ±45	89.3 ±11.81
16^{th}	7.67 ±7	97.74 ±1.91	1.67 ±1.37	99.52±0.725	Healed	100
20^{th}	2.83 ±3.19	99.18 ±1.31	Healed	Healed		

*mean±SD values

Figure 1.

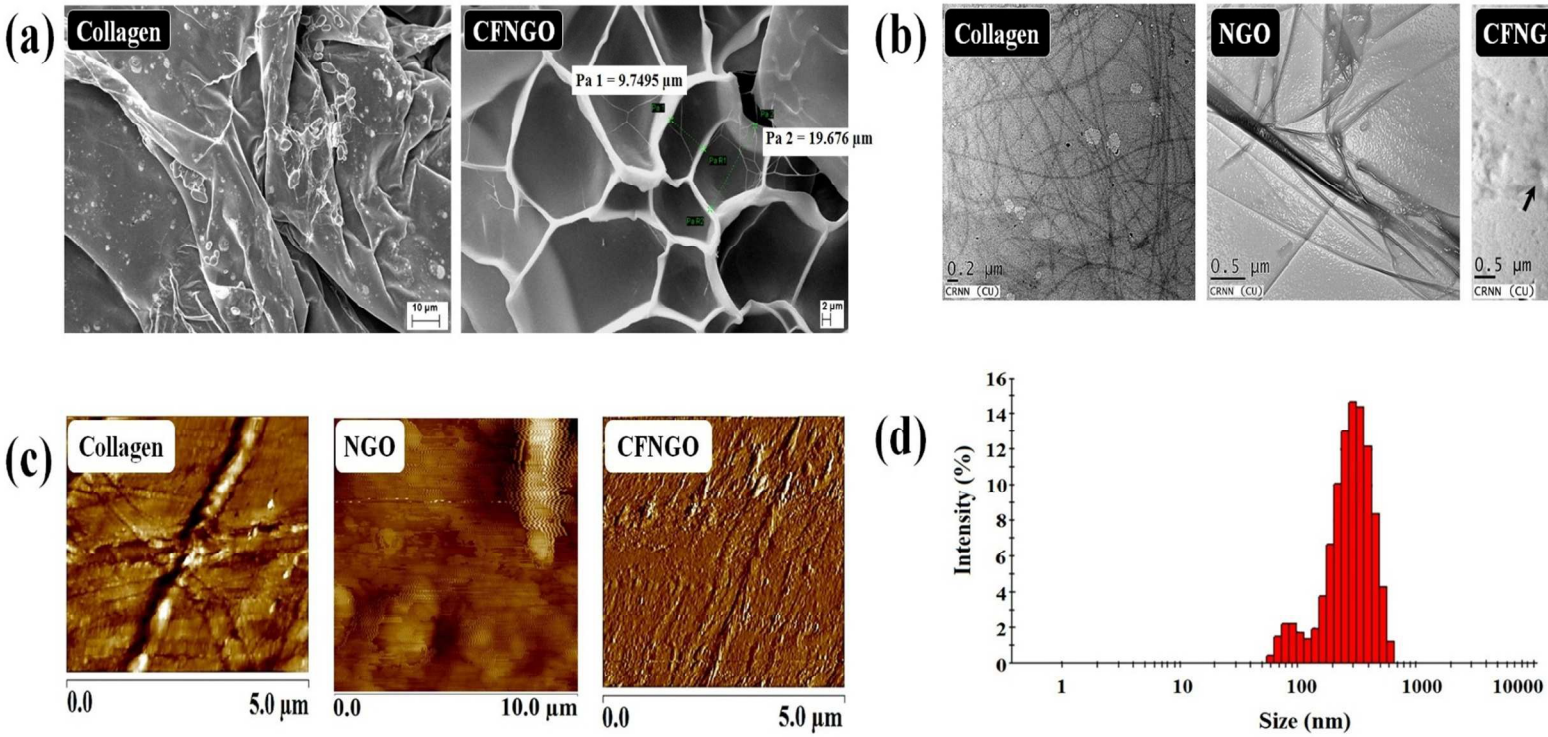

Figure 2.

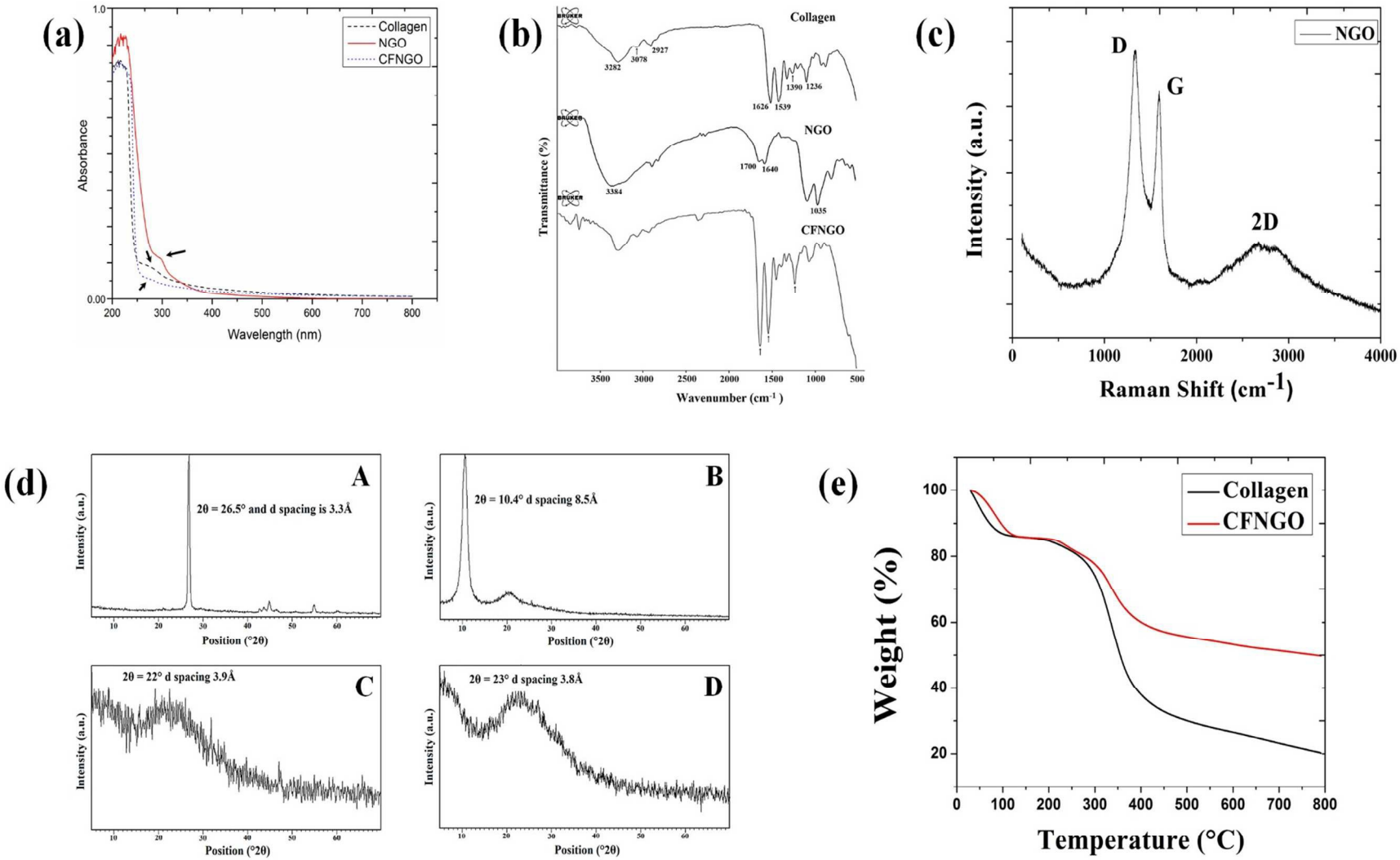

Figure 3.

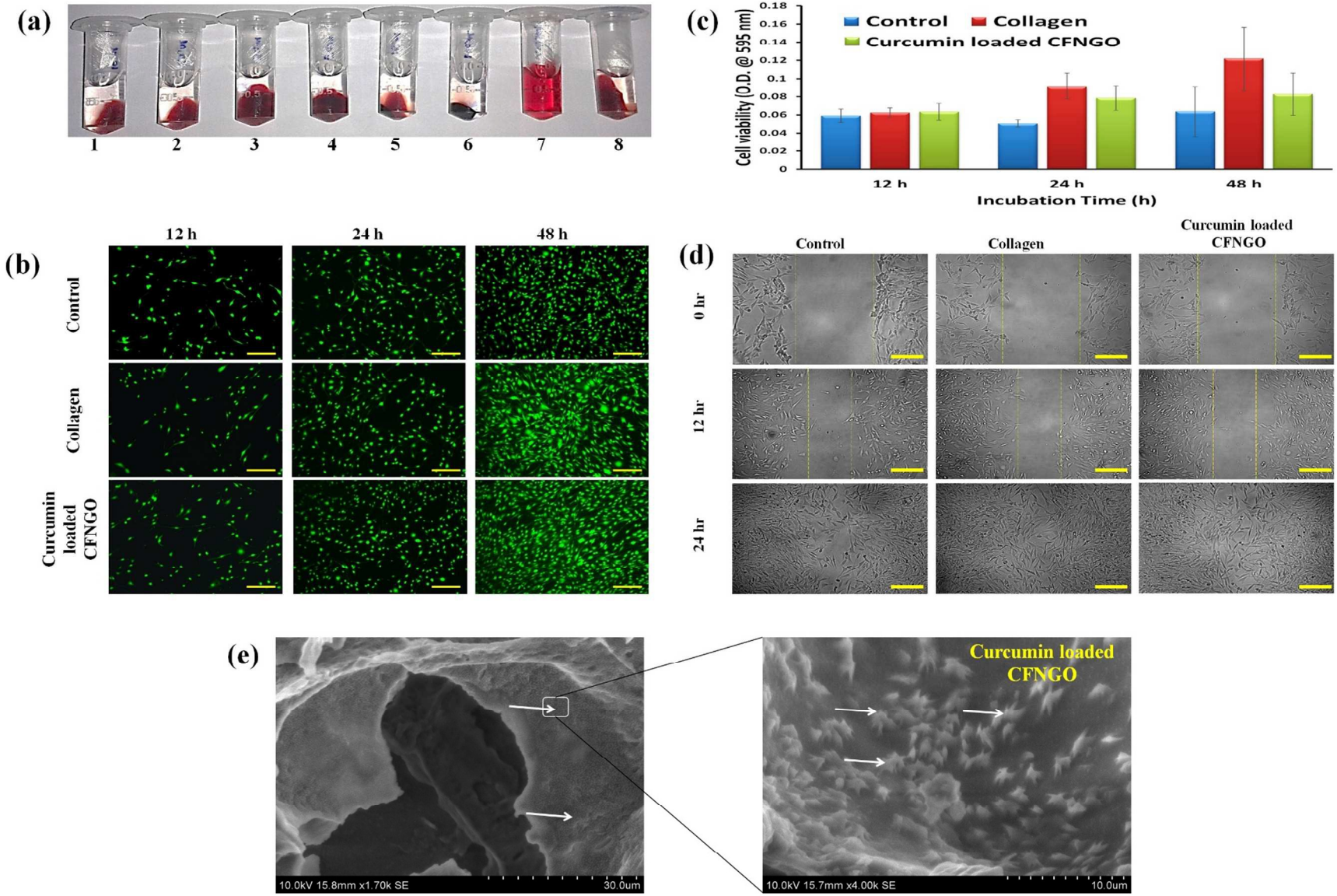

Figure 4.